Comparative Theoretical Study of Formaldehyde Decomposition on PdZn, Cu, and Pd Surfaces

Kok Hwa Lim,[†] Zhao-Xu Chen,[†,‡] Konstantin M. Neyman,[§] and Notker Rösch*[,†]

Department Chemie, Technische Universität München, 85747 Garching, Germany, Institute of Theoretical and Computational Chemistry, Department of Chemistry, Nanjing University, 210093 Nanjing, People's Republic of China, Institució Catalana de Recerca i Estudis Avançats (ICREA), 08010 Barcelona, Spain, and Departament de Química Física i Centre especial de Recerca en Química Teòrica, Universitat de Barcelona i Parc Científic de Barcelona, 08028 Barcelona, Spain

Received: March 7, 2006; In Final Form: June 6, 2006

Methanol steam reforming, catalyzed by Pd/ZnO (PdZn alloy), is a potential source of hydrogen for on-board fuel cells. CO has been reported to be a minor side product of methanol decomposition that occurs in parallel to methanol steam reforming on PdZn catalysts. However, fuel cells currently used in vehicles are very sensitive to CO poisoning. To contribute to the understanding of pertinent reaction mechanisms, we employed density functional slab model calculations to study the decomposition of formaldehyde, a key intermediate in methanol decomposition and steam reforming reactions, on planar surfaces of Pd, Cu, and PdZn as well as on a stepped surface of PdZn. The calculated activation energies indicate that dehydrogenation of formaldehyde is favorable on Pd(111), but unfavorable on Cu(111) and PdZn(111). On the stepped PdZn(221) surface, the dehydrogenation process was calculated to be more competitive to formaldehyde desorption than on PdZn(111). Thus, we ascribe the experimentally observed small amount of CO, formed during steam reforming of methanol on the Pd/ZnO catalyst, to occur at metallic Pd species of the catalyst or at defect sites of PdZn alloy.

1. Introduction

With increasing efficiencies, power densities, and decreasing cost, fuel cells have become a more environmentally friendly, realistic alternative to combustion engines.[1] Steam reforming of methanol (CH_3OH), $CH_3OH + H_2O \rightarrow H_2 + CO_2$, is considered to be an attractive option for producing H_2 in situ for on-board fuel cells, because of the simple handling and the low cost of this fuel.[1] Common catalysts for this reaction, based on Cu/ZnO, allow one to achieve nearly complete conversion of methanol to carbon dioxide (CO_2) at temperatures typically above 200 °C and at high pressure. Unfortunately, because of metal sintering, this type of catalyst is unstable at temperatures starting at ∼330 °C. Novel Pd/ZnO catalysts exhibit improved thermal stability and thus are more suitable for portable hydrogen production.[1] The high performance of Pd/ZnO catalysts was assigned to the formation of PdZn alloy particles,[2−4] and the (1:1) PdZn alloy was identified as an active component.[5] The direct effect of the ZnO support on the methanol steam reforming reactions over Pd/ZnO catalysts is minor as concluded from the experimental findings that (i) ZnO itself is unreactive[6] and (ii) the steam reforming activity of the ZnO-free catalysts, Zn−Pd/C, is similar to that of Pd/ZnO catalysts.[7]

On the PdZn alloy catalyst, methyl formate, H_2, and a small amount (4.8%) of carbon monoxide (CO) were shown to be produced during methanol decomposition; under steam reforming conditions, 0.8% CO was formed.[6] Pfeifer et al. reported that, during methanol steam reforming, CO is produced via methanol decomposition and not from CO_2 through the reverse water gas shift reaction.[4] Similar distributions of methanol decomposition and steam reforming products were obtained over monometallic Pd and alloy PdZn catalysts, when methanol as reactant was replaced by formaldehyde (CH_2O).[6] This suggests that formaldehyde is a crucial intermediate in the above methanol reactions. Thus, for a comprehensive understanding of methanol steam reforming, it is important to clarify the decomposition of CH_2O. Note that fuel cells currently used in vehicles are very sensitive to poisons, especially to CO, which has a detrimental effect on the performance of a fuel cell even at low (parts per million) concentrations.[8]

Recently, we have started systematic electronic structure investigations, using a density functional (DF) method, to better understand the structure of PdZn alloy catalyst[9−12] and its reactivity with respect to the initial phase of methanol steam reforming.[13−15] Thus far, we focused on elementary steps of methoxide (CH_3O) decomposition[13−15] as it is widely assumed to be the rate-limiting step of methanol steam reforming.[16] In the present work, we will continue these comparative investigations with the dehydrogenation of formaldehyde and formyl (CHO) on the surfaces Pd(111), Cu(111), PdZn(111), and PdZn-(221). To the best of our knowledge, no calculated activation energies of C−H bond breaking of formaldehyde on PdZn are available. The reaction energy of CH_2O and CHO dehydrogenation and the activation energy of CHO dehydrogenation on Cu(111)[17] and Pd(111)[18] have been addressed with the help of DF studies using periodic slab (PW91[19] functional) and cluster (BP[20,21] functional) models, respectively. The present systematic study provides insight into why CO is commonly not formed or is formed only in very small amounts during methanol dehydrogenation on PdZn and Cu based catalysts. These results lead to recommendations regarding the preparation of catalysts

* Corresponding author. Fax +49-89-2891 3468. E-mail roesch@ch.tum.de.
[†] Technische Universität München.
[‡] Nanjing University.
[§] ICREA and Universitat de Barcelona i Parc Científic de Barcelona.

10.1021/jp061410y CCC: $33.50
Published on Web 07/11/2006

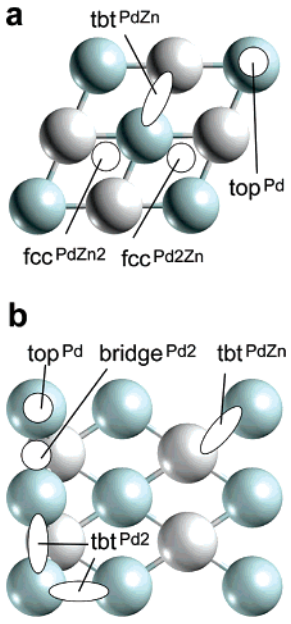

Figure 1. Top view of adsorption sites studied on the surfaces PdZn-(111) (a) and PdZn(221) (b). Atomic spheres: light blue, Pd; gray, Zn.

for methanol steam reforming that will allow one to achieve even lower concentrations of the byproduct CO.

The paper is organized as follows. In section 2, we describe the computational method and the models employed. In section 3, we discuss adsorption complexes of carbon monoxide, hydrogen, formaldehyde, and formyl on the four substrates under scrutiny. In section 4 we present structural data on adsorption systems pertinent to the two consecutive dehydrogenation steps of formaldehyde, yielding first formyl and then CO. Section 5 deals with the reaction and activation energies of these processes. In section 6, we will present our conclusions.

2. Models and Computational Details

The adsorbed moieties were placed on one side of four-layer slabs that model surfaces of Pd, Cu, and PdZn. For the (111) surfaces, we assumed a 2×2 surface unit cell comprising four metal atoms per layer (Figure 1a). All metal atoms were kept fixed at their optimized bulk truncated geometry for subsequent adsorption and reaction studies on the (111) surfaces; this simplification allows one to obtain results of sufficient accuracy for the purpose of the present study.[13] The PdZn(221) surface with exposed Pd steps[15] was represented by four layers of (111) orientation, with eight atoms per layer in each unit cell (Figure 1b). The two "top" stepped layers of the clean PdZn(221) surface (without an adsorbate) were relaxed, whereas the two "bottom" layers were kept fixed at the optimized truncated-bulk geometry.[9] The substrate atoms were fixed at this relaxed geometry during the subsequent geometry optimization of adsorption complexes and the location of transition state structures on the relaxed side of the slab. These models have previously been justified for our purpose.[13,15] The periodically repeated slabs were separated by a vacuum spacing larger than 1 nm.

For the PdZn(111) substrate,[13−15] we found that the ensemble effect on the adsorption energy at hollow sites (the nature of the metal atoms that make up the hollow site, i.e., Pd_2Zn vs $PdZn_2$) is considerably larger than the ligand effect (face-centered cubic (fcc) vs hexagonal close-packed (hcp) hollow sites).[13] In the following, we will restrict ourselves to study solely the ensemble effect on adsorption. Sites located directly at step edges of the PdZn(221) surface or in their immediate vicinity are affected by low-coordinated metal atoms and thus are more active than sites on the (111) terraces; therefore, we focused only on step sites of PdZn(221) when searching for preferred configurations of the adsorption complexes.[15] The adsorption sites studied on the (111) and (221) surfaces of PdZn alloy are sketched in Figure 1.

The calculations were performed with the plane-wave based Vienna ab initio simulation package (VASP)[22−24] using the PW91 generalized-gradient approximation for the exchange-correlation (xc) functional.[19] The interaction between atomic cores and electrons was described by the projector augmented wave method.[25,26] For integration over the Brillouin zone, we combined a $5 \times 5 \times 1$ Monkhorst−Pack grid[27] with a generalized Gaussian smearing technique.[28] Throughout we adopted an energy cutoff of 400 eV. All atomic coordinates of the adsorbates were optimized until the force acting on each atom was less than 0.1 eV/nm. We invoked a normal-mode analysis, restricted to the motion of the adsorbates, to confirm that the most stable adsorption configurations (and those chosen by us as initial states for our reaction studies) are indeed local minima.

The energy of adsorption, $\Delta E_{ad} = E_{ad/sub} - (E_{ad} + E_{sub})$, was calculated by subtracting the sum of the total energies of the adsorbate in the gas phase, E_{ad}, and of the clean substrate, E_{sub}, from the total energy, $E_{ad/sub}$, of the slab covered with the adsorbate in the optimized geometry. With this definition, a negative value of ΔE_{ad} implies a release of energy (favorable adsorption).

We located transition states (TS) with the nudged elastic band method.[29] Each TS structure was characterized by a normal-mode analysis to ensure that it features exactly one imaginary frequency. Further computational details can be found elsewhere.[13,15]

3. Adsorption Complexes

In previous studies,[13,15] we provided comprehensive information on adsorption complexes of carbon monoxide, hydrogen, and formaldehyde at surfaces of Pd and Cu metals and PdZn alloy. In the following, first we will briefly describe the most relevant features of these adsorption systems and then we will focus on the adsorption of formyl on the three substrates.

3.1. Carbon Monoxide. CO adsorbs on the hollow site of Pd(111) with basically no preference for either fcc or hcp threefold sites; the energy of adsorption is calculated at about -178 kJ mol^{-1}.[13] The adsorbate interacts notably weaker with Cu(111), about -82 kJ mol^{-1}, also on hollow sites.[13] A somewhat stronger interaction, -96 kJ mol^{-1}, is calculated on the (111) surface of PdZn alloy, where CO was determined to be most stable on top of Pd atoms, i.e., at top^{Pd} sites.[13] On PdZn-(221), CO also prefers Pd sites, namely top^{Pd} sites at step edges, with an energy of adsorption of -124 kJ mol^{-1}; however, adsorption complexes of CO on edge bridge^{Pd2} sites are almost as stable, with an energy of adsorption ΔE_{ad} at -120 kJ mol^{-1}. Thus, the more active Pd atoms at the step positions of PdZn-(221) stabilize the adsorption of CO by 28 kJ mol^{-1} compared to the planar PdZn(111) surface.

3.2. Hydrogen. As on many other metal surfaces,[30] atomic hydrogen on the (111) surfaces of Pd and Cu metals and PdZn alloy tends to occupy sites with higher coordination: adsorption of atoms H on threefold hollows is energetically favored on all three substrates. Atomic hydrogen essentially does not show any preference between fcc and hcp sites on Pd(111) and Cu-(111), and the calculated energies of adsorption on these two

TABLE 1: Calculated Characteristics[a] of the Most Stable Adsorption Complexes of CHO on Pd, Cu, and PdZn Surfaces

	Pd(111) η^1(C)-top	Cu(111) η^1(C)-fcc	PdZn(111) η^2(C,O)-tbt^{PdZn}	PdZn(221) η^2(C,O)-tbt^{Pd2}
C−O	120	122	125	123
C−M	199	215	205[b]	201[b]
O−M	288	280	225[c]	234[b]
z(C)	198	156	188	181
ΔE_{ad}	−214	−127	−167	−186

[a] Interatomic distances C−O, C−M, and O−M (M is a substrate metal atom), height z(C) of atom C over the top crystal plane of the substrate (all distances in picometers), and energy of adsorption ΔE_{ad} [in kJ mol^{-1}; a negative sign implies an energy release, i.e., favorable adsorption, see section 2]. [b] M = Pd. [c] M = Zn.

substrates are about −270 and −237 kJ mol^{-1}, respectively.[13] On PdZn(111), H atoms prefer the hollow sites Pd_2Zn, by at least 20 kJ mol^{-1}, over the next stable site, $PdZn_2$ hollows. The Pd_2Zn sites, offering a higher coordination by Pd centers, feature an energy of adsorption of −249 kJ mol^{-1}.[13] On PdZn(221), our calculations favor H adsorption on a bridge^{Pd2} site at the step edge, with ΔE_{ad} = −253 kJ mol^{-1}.[15]

3.3. Formaldehyde. The most stable adsorption complexes of CH_2O on the considered surfaces of Pd, Cu, and PdZn feature a top−bridge−top (tbt) configuration, where the C and O atoms each are bridging two substrate atoms. Formaldehyde forms only weak adsorption bonds with the (111) surfaces of Pd (−43 kJ mol^{-1}), Cu (−11 kJ mol^{-1}), and PdZn (−23 kJ mol^{-1}).[13] On PdZn(221), the adsorption energy is 20 kJ mol^{-1} larger (by absolute value) than that on PdZn(111),[15] reaching the same value as obtained for Pd(111).

3.4. Formyl. CHO is an intermediate of formaldehyde dehydrogenation. Table 1 presents the geometric parameters and energies of adsorption calculated for the most stable adsorption complexes of CHO on the surfaces of Pd, Cu, and PdZn. CHO species bind to these substrates either via the carbon atom in η^1(C) configuration (Cu, Pd—where the CHO moiety forms a V-shape structure with the C atom close to the surface) or simultaneously via both C and O atoms in η^2(C,O) configuration (PdZn—where the molecular plane is perpendicular to and the C−O bond is essentially parallel to the surface).

According to our calculations, formyl does not exhibit a clear site preference on Pd(111); energies of adsorption at the various sites studied differ by less than 15 kJ mol^{-1} and the largest value (in absolute terms) is calculated for the configuration η^1-(C) at on-top sites [r(C−Pd) = 199 pm and r(C−O) = 120 pm], with ΔE_{ad} = −214 kJ mol^{-1} (PW91 xc functional, Table 1). In earlier cluster model studies[18] (BP xc functional) hollow sites were determined to be favored on Pd(111), with the energy of adsorption at −340 kJ mol^{-1}. More recent periodic calculations by the same group (using a slab model of three layers) resulted in an energy of adsorption at −237 kJ mol^{-1} (PW91 xc functional).[31] The differences of our data from those of the previous slab model study are most likely due to the fact that the three-layer model used earlier does not allow one to achieve converged results; in the case of a rather flat nature of the potential energy surface (PES), as for CHO on Pd(111), a more sophisticated model can lead to a different site preference (Table 1). The situation is reminiscent of CHO on Pt(111) where two separate DF studies, employing even the same slab thickness (three layers) and the same xc functional PW91, but slightly different substrate geometries and surface relaxation approaches, claimed the top configuration (ΔE_{ad} = −228 kJ mol^{-1})[32] as well as the fcc configuration (ΔE_{ad} = −237 kJ mol^{-1})[31] as most stable, at the two low surface coverage values of 1/9 and 1/4, respectively. Similar to Pd(111), we found that CHO shows essentially no preference for binding sites on the Cu(111) surface; the strongest interaction, ΔE_{ad} = −127 kJ mol^{-1}, is at the fcc site. Cluster model calculations had identified the bridge site as most favored on Cu(111), with ΔE_{ad} = −140 kJ mol^{-1}, while hollow sites were characterized by a B3LYP energy of adsorption of about −110 kJ mol^{-1}.[33] However, this preference of the bridge site is likely a cluster artifact, reminiscent of the case on the Pd(111) surface. In fact, just as in the present study, recent PW91 calculations also based on periodic slab models furnished essentially degenerate η^2(C,O) tbt and η^1(C) hollow configurations of formyl adsorbed on Cu(111),[17] with ΔE_{ad} of about −110 kJ mol^{-1}. According to the present work, the fcc site is slightly more favorable on Cu(111) (Table 1), at variance with Pd(111). This difference is due to the different nature of CHO interactions with Cu (s metal) and Pd (d metal), reminiscent of methyl adsorption.[13] Recall that CHO binds to the Cu and Pd surfaces in the same η^1(C) configuration as CH_3. For the latter substrate, it was shown that the 2σ molecular orbital of CH_3 interacts with a transition metal substrate (M) and that this 2σ−d(M) bonding results in the preference of on-top sites, whereas 2σ−s(M) favors adsorption complexes at hollow sites.[34]

Not surprisingly, adsorbed CHO also exhibits a flat PES on PdZn. On PdZn(111), the tbt^{PdZn} site was calculated to feature the largest energy of adsorption (in absolute terms) ΔE_{ad} = −167 kJ mol^{-1}, in the η^2(C,O) configuration [r(C−Pd) = 205 pm, r(O−Zn) = 225 pm; Table 1]. On the PdZn(221) surface, formyl also prefers to adsorb in the η^2(C,O) mode. However, there the adsorbate binds to two Pd edge atoms in the tbt^{Pd2} configuration, in contrast to one Pd atom and one Zn atom in the adsorption complex at PdZn(111). Similar to the cases of adsorbed CH_2O and CO (see above),[13,15] the more active Pd atoms at the step edges strengthen the binding of CHO, with ΔE_{ad} = −186 kJ mol^{-1} (Table 1). This value is ∼20 kJ mol^{-1} more negative than that calculated for the complexes at terrace sites of PdZn(111). In the top^{Pd} configuration on PdZn(221), CHO is only slightly less stable, by 6 kJ mol^{-1}.

In summary, the PES of formyl on all substrates under scrutiny is rather flat, with binding energies that vary less than 15 kJ mol^{-1} across all sites studied. Therefore, under reaction conditions one expects CHO to be very mobile on these surfaces. Of the substrates studied, formyl binds the least strongly on Cu(111), ΔE_{ad} ∼ −125 kJ mol^{-1}, and the strongest on Pd(111), ΔE_{ad} ∼ −215 kJ mol^{-1}. On the alloy surface PdZn(111), the energy of adsorption is intermediate, ΔE_{ad} ∼ −165 kJ mol^{-1}, between the values calculated for Pd(111) and Cu(111). Thus, the situation is qualitatively similar to those of all other adsorbates we previously considered.[13]

4. Structures Involved in Decomposition of Formaldehyde

As formaldehyde is weakly adsorbed and formyl shows essentially no preference for a particular adsorption site, we carried out a normal-mode analysis of the adsorption structures of formaldehyde and formyl that were chosen as initial states (IS) of dehydrogenation, thus ensuring that the initial states were at least local minima.

4.1. Dehydrogenation of Formaldehyde. The most stable adsorption configuration of formaldehyde, tbt, was chosen as the IS for the dehydrogenation reaction. In the IS on Pd(111), the oxygen atom of CH_2O binds to the Pd atom at a distance of 211 pm and the shortest C−Pd distance is 215 pm. The C−O bond, 131 pm, is almost parallel to the (111) surface. On Pd-(111), in the final state (FS), CHO + H_a (H_a is the H atom split

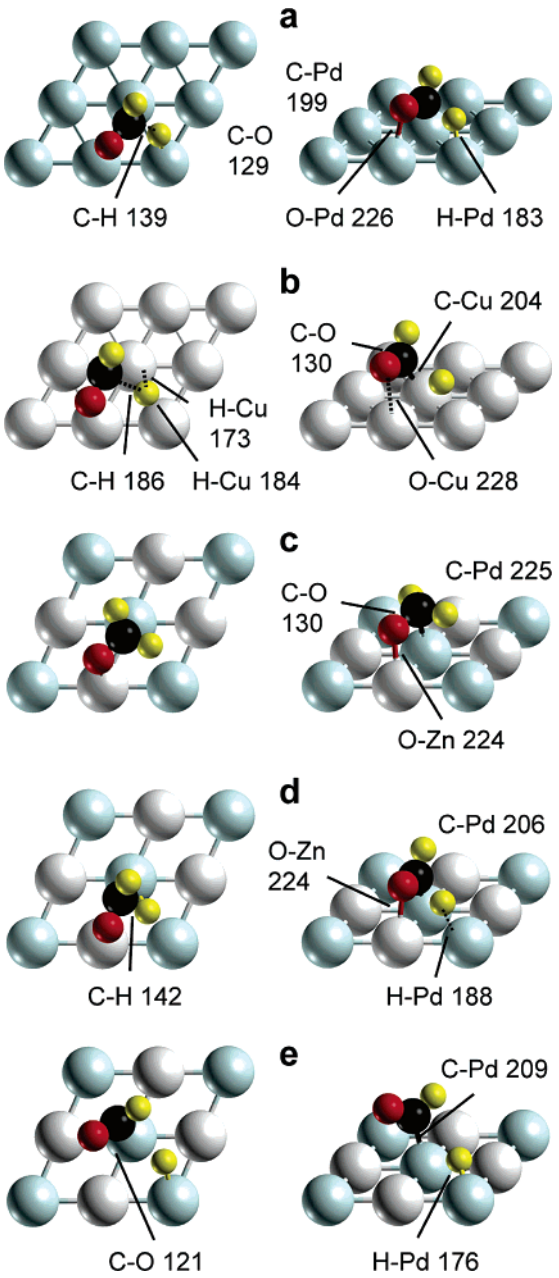

Figure 2. Top (left-hand panels) and side views (right-hand panels) of calculated structures involved in the C−H bond breaking of formaldehyde: (a) TS on Pd(111), (b) TS on Cu(111), (c) IS on PdZn-(111), (d) TS on PdZn(111), and (e) FS on PdZn(111). Bond lengths in picometers. Atomic spheres: light blue, Pd; gray, Zn/Cu; red, O; black, C; yellow, H.

off and located at an fcc site), formyl resides on top with the carbon atom bound to a Pd atom. As already mentioned, this is the most stable configuration of CHO on Pd(111).

On the way to the transition state (TS) of C−H bond breaking on Pd(111), the C−H_a bond (with H above C) rotates around the C−O axis and is stretched by moving the H_a atom toward a bridge site. The CHO moiety remains at the tbt site, with the C−Pd distance shortened and the O−Pd bond elongated to 226 pm, hence weakened. This, in turn, strengthens to some extent the C−O bond which shortens from 131 pm in the IS to 129 pm in the TS (Figure 2a). In the TS, the formyl species is close to a tbt site, with the shortest H_a−Pd distance at 183 pm. The distance C−Pd, 199 pm, is 16 pm shorter than in the IS. The C−H_a bond is elongated from 111 pm in the IS to 139 pm in the TS. Past the TS, the atom H_a retreats to a favorable fcc site.

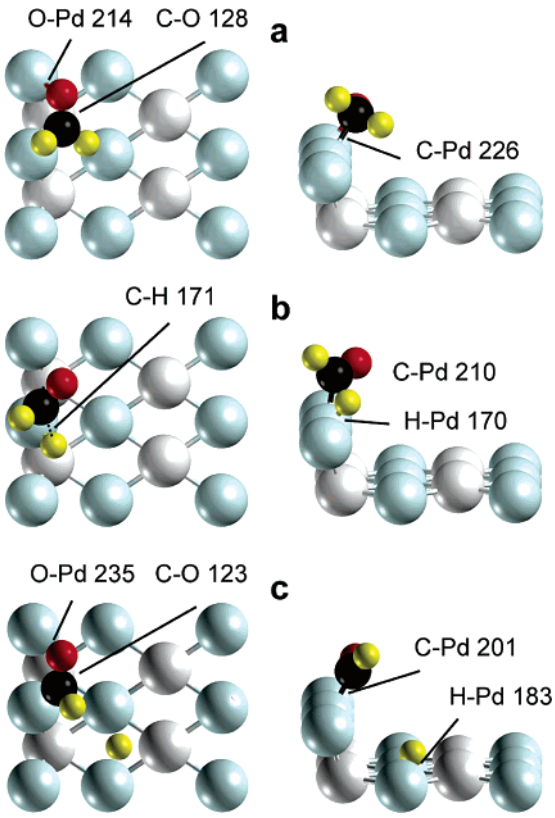

Figure 3. Top (left-hand panels) and side views (right-hand panels) of calculated structures involved in the C−H bond breaking of formaldehyde: (a) IS, (b) TS, and (c) FS on PdZn(221). Bond lengths in picometers. Atomic spheres: light blue, Pd; gray, Zn; red, O; black, C; yellow, H.

In the FS, formyl is close to the on-top site, with r(C−Pd) = 197 pm and r(C−O) = 122 pm.

The dehydrogenation of formaldehyde on Cu(111) occurs in a similar way, and the shape of the TS structure resembles that on Pd(111), except that on Cu it is a late transition state with a significantly longer C−H_a distance, 186 pm (Figure 2b). Other structural characteristics are quite similar: r(C−O) = 130 pm, r(C−Cu) = 204 pm, and r(H_a−Cu) = 173 and 184 pm. Another slight difference is that the formyl moiety favors a threefold hollow site on Cu(111), instead of the top site on Pd(111) (Table 1). Thus, the resulting CHO species moves from the tbt site in the TS to a hollow site in the FS with r(C−Pd) = 215 pm and r(C−O) = 119 pm.

The IS of CH_2O dehydrogenation on PdZn(111) is a tbt^{PdZn} configuration with r(O−Zn) = 224 pm and r(C−Pd) = 225 pm (Figure 2c). The C−H_a bond breaking process is rather similar to the corresponding reactions on the (111) surfaces of Pd and Cu. The TS structure resembles that on Pd(111) with a C−H_a distance of 142 pm, while r(C−Pd) = 206 pm and r(O−Zn) = 224 pm (Figure 2d). In the FS (Figure 2e), the dissociated H_a atom bound close to a fcc^{PdZn2} site pushes the formyl moiety from the most favorable tbt^{PdZn} site (Table 1) to a top^{Pd} site, with r(C−Pd) = 209 pm and r(C−O) = 121 pm.

On PdZn(221) (Figure 3), we chose the tbt^{Pd2} configuration as IS; in that adsorption complex both C and O atoms are bound to Pd centers at the step edge, with r(O−Pd) = 214 pm and r(C−Pd) = 226 pm. C−H_a bond breaking of CH_2O starts with its rotation about the C−O axis, where one H center moves above the C atom and H_a is stretched toward the $bridge^{Pd2}$ site. In the TS, the formyl moiety is near a top^{Pd} site with r(C−Pd) = 210 pm and r(C−H_a) = 171 pm. Past the TS, the atom H_a

retreats to a terrace hollow site and CHO moves to a tbt^{Pd2} site with r(C−Pd) = 201 pm, r(C−O) = 123 pm, and r(O−Pd) = 235 pm. When we studied the decomposition of CH_3O,[15] locating the dissociated atom H_a on the upper terrace of a PdZn-(221) step changed the height of the barrier by only 4 kJ mol^{-1} compared to a position of H_a on the lower terrace. For the barrier of H abstraction from formaldehyde and formyl, one can expect a similarly small variation with the FS location of the abstracted H_a on the upper or lower terrace.

4.2. Dehydrogenation of Formyl. Based on our findings that the PES of adsorbed CHO is flat on the addressed surfaces of Pd, Cu, and PdZn, we chose the top adsorption configuration on all substrates as the IS for our comparative study of formyl dehydrogenation. In this way, the estimated activation energies on Cu(111) and PdZn(111) are lowered because the corresponding initial states are not the most stable structures. However, due to the flat character of the PES, these differences amount to only ∼10 kJ mol^{-1}. An advantage is that this strategy enables a direct comparison of analogous reaction paths for the four substrates studied. CO species in the FS systems reside at fcc sites on Pd(111) and Cu(111) as well as on top of a Pd atom at PdZn(111) and PdZn(221), the most stable structures for CO on these substrates.[13] In these FS complexes, the atom H_a split off resides at an fcc site remote from CO.

On Pd(111), hydrogen abstraction from CHO starts with the IS moiety sliding from the top site to an fcc site. In the course of the reaction, the H−Pd distance decreases, manifesting a corresponding bonding interaction. In the TS (Figure 4a), the activated C−H bond is elongated by 15 pm to 127 pm; the C−O and C−Pd distances are calculated at 118 and 204 pm, respectively. In fact, in the TS, CO and H "share" a Pd center. Therefore, bonding competition[35] pushes the H fragment away to another fcc site. In the FS, the product CO resides at an fcc site with the C−O axis perpendicular to the surface, with r(C−Pd) = 210 pm and r(C−O) = 119 pm.

Formyl dehydrogenation on Cu(111) is similar to that on Pd-(111). In the TS (Figure 4b), the C−H bond (137 pm) is activated by one Cu atom. The H atom is near an hcp site with r(H−Cu) = 181 pm and r(C−Cu) = 204 pm. In the FS, the atom H is located at an fcc site, with r(H−Cu) = 172 pm, while the CO moiety resides at another fcc site with r(C−Cu) = 207 pm and r(C−O) = 118 pm.

In contrast to Pd(111) and Cu(111), on PdZn(111) C−H bond scission of CHO begins with an inclination of the formyl moiety, with H pointing toward another Pd atom of the top^{Pd} adsorption site (Figure 4c). That H−Pd distance shrinks to 211 pm in the TS, indicating the beginning of a bonding interaction. In the TS on PdZn(111) (Figure 4c), the C−H distance is stretched rather far, to 176 pm, while the CO moiety is almost at a top site, with r(C−O) = 120 pm and r(C−Pd) = 210 pm. Once the C−H bond is broken, the H atom moves to an fcc^{PdZn2} hollow site with r(H−Pd) = 172 pm and r(H−Zn) = 197 pm in the FS (Figure 4d). CO stays at the top^{Pd} site with the C−O axis perpendicular to the surface, with r(C−Pd) = 194 pm and r(C−O) = 115 pm.

In the TS of formyl dehydrogenation on PdZn(221) (Figure 5), the C−H bond (148 pm) is activated by a Pd atom, similarly to the TS on Pd(111). The H atom is near a bridge^{Pd2} site with r(H−Pd) = 179 pm and r(C−Pd) = 200 pm. In the FS, the atom H is located at a terrace hollow site, while the CO moiety resides at a top^{Pd} site with r(C−Pd) = 194 pm and r(C−O) = 116 pm.

In summary, the TS structures of hydrogen abstraction from formaldehyde and formyl on the substrates studied are rather similar, except for C−H bond breaking of formyl on PdZn-(111) surface, which occurs over two substrate Pd atoms. These similarities are mainly due to the similar adsorption modes of the IS; recall that formaldehyde prefers a tbt configuration on all these surfaces and formyl lacks any preferences for an adsorption site. The produced atomic hydrogen always prefers hollow sites.

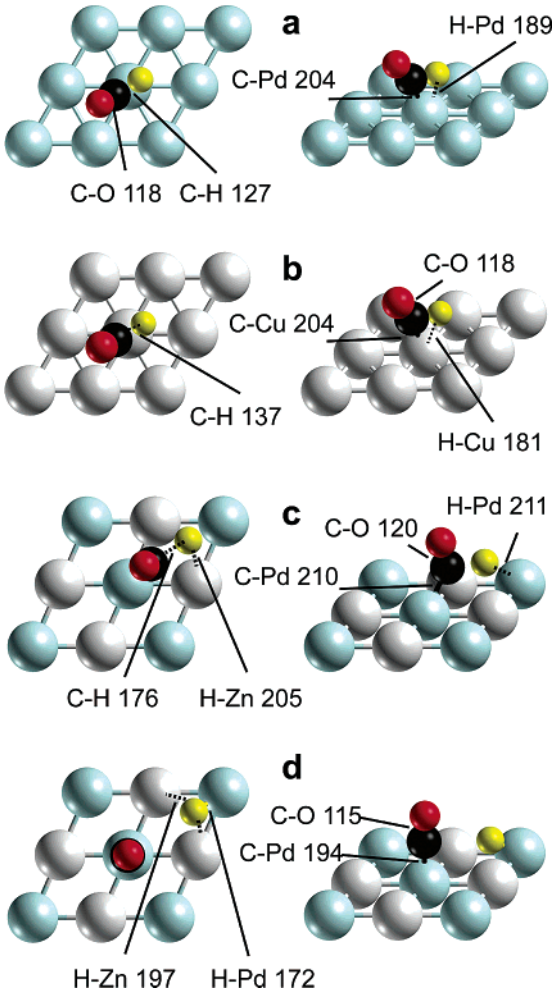

Figure 4. Top (left-hand panels) and side views (right-hand panels) of calculated structures involved in the C−H bond breaking of formyl: (a) TS on Pd(111), (b) TS on Cu(111), (c) TS on PdZn(111), and (d) FS on PdZn(111). Bond lengths in picometers. Atomic spheres: light blue, Pd; gray, Zn/Cu; red, O; black, C; yellow, H.

5. Reaction and Activation Energies of Formaldehyde Decomposition

Table 2 and Figure 6 display the kinetic and thermodynamic data calculated for formaldehyde dehydrogenation on Pd and Cu metals and on PdZn alloy, first to formyl and then to CO. We also present a summary of our previous results on the conversion of methoxide to formaldehyde.[13−15] In Figure 6, we chose a CH_2O molecule in the gas phase plus a clean substrate as energy reference. Zero-point-energy corrections were calculated to lower the activation energies by 13−19 kJ mol^{-1} (Table 2), mainly because a stiff C−H vibrational mode of the IS (adsorbed CH_2O and CHO), ∼2800 cm^{-1}, is lacking in each of the C−H bond breaking transition states.

On Pd(111), we calculated H abstraction from CH_2O to be exothermic, −56 kJ mol^{-1}, in perfect agreement with the previously reported PW91 value of −55 kJ mol^{-1}.[31] On Cu-(111), the analogous reaction is endothermic; the present reaction

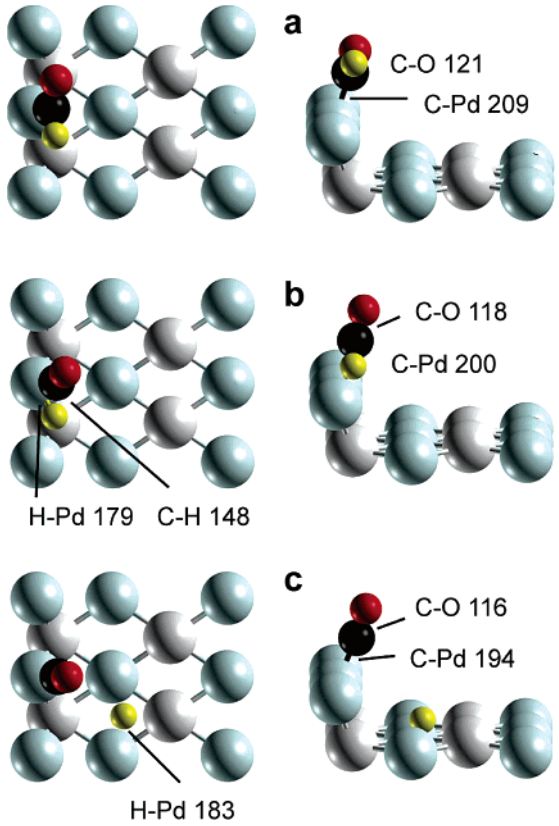

Figure 5. Top (left-hand panels) and side views (right-hand panels) of calculated structures involved in the C−H bond breaking of formyl: (a) IS, (b) TS, and (c) FS on PdZn(221). Bond lengths in picometers. Atomic spheres: light blue, Pd; gray, Zn; red, O; black, C; yellow, H.

TABLE 2: Calculated Activation Energies E_a and Reaction Energies E_r of Formaldehyde and Formyl Dehydrogenation on Pd, Cu, and PdZn Surfaces (in kJ mol^{-1})[a]

	$CH_2O \rightarrow CHO + H$		$CHO \rightarrow CO + H$	
	E_a	E_r[b]	E_a	E_r[b]
Pd(111)	38 (22)	−56 (−65)	60 (41)	−132 (−141)
Cu(111)	80 (63)	36 (25)	31 (16)	−86 (−93)
PdZn(111)	78 (64)	−4 (−18)	44 (25)	−71 (−80)
PdZn(221)	76 (63)	−7 (−17)	41 (22)	−84 (−94)

[a] Values in parentheses corrected for zero-point energy. [b] The heat of reaction E_r is calculated as $E_r = -\sum(\Delta E_{ad,R}) + (\sum E_P - \sum E_R) + \sum(\Delta E_{ad,P})$. $\sum E_P$ and $\sum E_R$ are sums of the total energies of the products P and the reactants R, respectively, in the gas phase. $\sum(\Delta E_{ad,P})$ and $\sum(\Delta E_{ad,R})$ are the sums of the energies of adsorption of isolated product and reactant species, respectively. A positive value of E_r characterizes an endothermic reaction; see section 2.

energy of 36 kJ mol^{-1} is compared to 54 kJ mol^{-1} reported previously.[17] The desorption of formaldehyde ($\Delta E_{ad} = -11$ kJ mol^{-1}) from this surface is energetically less demanding than H abstraction. On the (111) and (221) surfaces of PdZn, H abstraction from CH_2O is essentially thermoneutral, with reaction energies of −4 and −7 kJ mol^{-1}, respectively.

The activation energy for H abstraction from CH_2O on Pd(111) was calculated at 38 kJ mol^{-1} (Table 2, Figure 6), compared to ∼10 kJ mol^{-1} calculated for the more active surface Pt(111).[32] As H abstraction from formaldehyde on Cu(111) requires more energy than the desorption of the reactant, we refrain from considering the abstraction of H in detail. Nevertheless, we computed the activation barrier of CH_2O dehydrogenation on Cu(111) for comparison with the analogous process on PdZn and for gaining insight into an elementary step, CHO + H → CH_2O, of methanol synthesis on Cu(111). The calculated activation barrier of CH_2O dehydrogenation to CHO on Cu(111), 80 kJ mol^{-1}, is essentially the same as that on PdZn(111), 78 kJ mol^{-1}, and on PdZn(221), 76 kJ mol^{-1}. On the surfaces of PdZn, the activation barriers are about twice as high as they are on Pd(111), indicating drastically lower rates of H abstraction on the alloy. Even after zero-point-energy correction, the activation energies on the PdZn surfaces remain substantial, ∼64 kJ mol^{-1}. This value is notably larger than the energy required for the desorption of CH_2O from PdZn surfaces, 23−43 kJ mol^{-1}.[13,15] In other words, if formed on PdZn surfaces, formaldehyde is kinetically inclined to desorb rather than to undergo dehydrogenation.

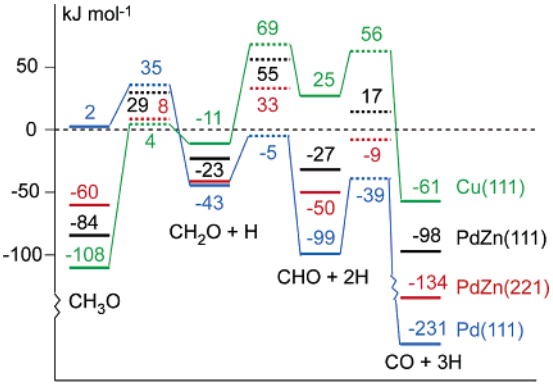

Figure 6. Calculated energetics (kJ mol^{-1}) of formaldehyde dehydrogenation to formyl and then to CO on Pd, Cu, and PdZn surfaces. A formaldehyde molecule in the gas phase and a clean substrate are chosen as the energy reference. For comparison, our previous results of methoxide conversion to formaldehyde are presented.[13−15] Dashed lines mark transition state energies (without zero-point-energy corrections).

According to our results, formyl dehydrogenation is exothermic on all the substrates scrutinized (Table 2). The calculated reaction energy on Pd(111) is −132 kJ mol^{-1} (−141 kJ mol^{-1} after zero-point correction); a previous DF study reported a value of −100 kJ mol^{-1}.[31] On Cu(111), the reaction energy is −86 kJ mol^{-1} (−93 kJ mol^{-1}), again differing notably from a published value, −67 kJ mol^{-1}.[17] Recall that these older results for Pd(111) and Cu(111) had been obtained for three-layer substrate models,[17,31] whereas in the present study four-layer models were used. On the PdZn surfaces, the calculated reaction energies, −71 kJ mol^{-1} (−80 kJ mol^{-1}) for PdZn(111) and −84 kJ mol^{-1} (−94 kJ mol^{-1}) for PdZn(221), are rather close to the present results calculated for Cu(111). Our test calculations showed[36] that the value of the adsorption energy may change by up to ∼10 kJ mol^{-1} when the thickness of the metal slab is increased from three to four layers.

We calculated rather low activation energies of formyl dehydrogenation on Pd(111), Cu(111), PdZn(111), and PdZn(221), namely 60, 31, 44, and 41 kJ mol^{-1}, respectively. For Pd(111), results of different TS structures, ranging from 18 to 90 kJ mol^{-1} with CHO at top configuration, have been obtained at the BP level from cluster models of varying size.[18] For Cu(111) a value of 17 kJ mol^{-1} is available from a DF PW91 slab model study.[17] The above-mentioned activation energies of the present work become even more favorable after a zero-point-energy correction which lowers the activation barriers by 13−19 kJ mol^{-1}. Our results reflect the strongly exothermic character of formyl dehydrogenation.

Interestingly, the activation energies of C−H bond breaking of CH_2O and CHO on step sites of PdZn(221) surface remain essentially unchanged compared to the planar surface PdZn(111). To rationalize these findings, we analyzed the energies

of adsorption ΔE_{ad} of the species involved in the IS and FS. On PdZn(221), in the IS of C−H cleavage, CH_2O is adsorbed 20 kJ mol^{-1} more strongly than on PdZn(111). In the FS on PdZn(221), CHO is bound 19 kJ mol^{-1} more strongly than on PdZn(111); likewise, H is adsorbed 4 kJ mol^{-1} more strongly on PdZn(221) than on PdZn(111). Therefore, the enhanced interactions of the species in the IS and FS basically cancel each other and result in closely similar reaction energies for formaldehyde dehydrogenation on PdZn(221) and PdZn(111). Our calculations reveal qualitatively the same situation also for the dehydrogenation of formyl.

Thus the situation is different from C−H bond cleavage of methoxide, for which we assigned the lower barrier on PdZn(221) compared to PdZn(111) to be a weaker binding of methoxide (reactant) and a stronger binding of formaldehyde (product) on PdZn(221), as compared to PdZn(111).[15] Therefore, the absence of significantly lower barriers for the dehydrogenation of CH_2O and CHO on PdZn(221) compared to the PdZn(111) surface does not come as a surprise; in particular note that the reactants, CH_2O and CHO, bind more strongly on PdZn(221) than on PdZn(111).

Our calculations show that complete dehydrogenation of formaldehyde on Pd(111) is both thermodynamically and kinetically favorable, in agreement with the experimental observation that methoxide decomposes to CO on Pd(111) surface.[37] On the Cu(111) surface, dehydrogenation of CH_2O to CHO is thermodynamically unfavorable compared to the reactant desorption process. This is in line with experimental evidence that the clean Cu(111) surface is inert with respect to molecular methanol, which is the only stable species identified there below its desorption at about 210 K.[38]

During methanol dehydrogenation on Pd/ZnO catalysts (PdZn alloy), a small amount of CO is produced (less than 5%).[4] In light of our finding that the overall dehydrogenation reaction of CH_2O is exothermic on PdZn, a small yield of CO is not unexpected. (When advancing this argument, we implicitly assume that our results for the catalyst model also hold for the real catalyst used in the experiment.) However, under reaction conditions kinetics appears to be important. Our calculations indicate that dehydrogenation of CH_2O on PdZn is kinetically unfavorable ($E_a = \sim 77$ kJ mol^{-1}) when compared to desorption [$\Delta E_{ad} = -23$ kJ mol^{-1} for PdZn(111), -43 kJ mol^{-1} for PdZn(221)].

As our data show, formaldehyde decomposes to CO on monometallic Pd. Indeed, Pd aggregates may be present on the "real" catalyst; i.e., some Pd may not have been converted to PdZn alloy.[39] Thus, when preparing the catalyst, care must be taken to ensure that alloying is complete, to prevent undesired CO formation while dehydrogenating CH_2O. Furthermore, "real" Pd/ZnO catalysts exhibit other intrinsic defect sites and/or impurities, at which formaldehyde may decompose. (In the present study, we did not address the scenario where Pd steps on Pd/ZnO catalysts are enriched with Zn atoms, as our earlier calculations had ruled out Zn enrichment of the PdZn(111) surface.[10] In any case, we do not expect such a change of the local stoichiometry of Pd steps to be crucial for the main conclusions of this work.) Although the barrier of formaldehyde C−H bond breaking on PdZn(221) was calculated to be comparable to that on PdZn(111) (Table 2), this process is more competitive to the desorption of formaldehyde than that on the PdZn(111) surface, because CH_2O adsorbs more strongly on PdZn(221) (see Figure 6).

The above conclusions for the two situations are in accord with the experimental observation. First, a high selectivity to CO_2 is achieved with 5−37.5% Pd loading of a ZnO support, used for oxidative methanol steam reforming (in the presence of oxygen). Also, one observes a notable yield of CO if the Pd loading is outside this range.[39] One can expect that, at high Pd loading, not all metallic Pd will be converted to PdZn alloy. At a low Pd loading, the crystallites of PdZn alloy are small, with an average diameter of ∼20 nm;[39] hence, catalysts may contain more defect sites (steps, edges, etc.) which may render the dehydrogenation of formaldehyde more competitive to the desorption process, similar to the case of PdZn(221). Because CO is an undesirable side product, it is important to optimize the Pd loading on the ZnO catalyst to ensure that dehydrogenation of CH_2O is suppressed on the Pd/ZnO catalyst for methanol steam reforming.

Finally, we would like to briefly discuss implications of our results for the initial steps of methanol synthesis. A mixture of CO (5%), CO_2 (5%), and H_2 (90%) is a common feedstock for methanol synthesis in industry.[40] Recently, Iwasa et al.[41] reported that hydrogenation of CO over Pd/ZnO (PdZn alloy) and Pd catalysts does not produce methanol—in contrast to the hydrogenation of CO_2 on Pd/ZnO and Cu/ZnO catalysts. On all three substrate materials studied in this work, the hydrogenation of CO to CHO is strongly endothermic, by at least 70 kJ mol^{-1}, and is characterized by a high activation energy of at least 100 kJ mol^{-1} (Figure 6). Even when CHO species are formed on the surface of the catalyst, their dehydrogenation is calculated to be kinetically and thermodynamically more favorable than further hydrogenation to CH_2O (or even to CH_3O), in line with observations[41] that methanol is not formed on Pd and Pd/ZnO catalysts during CO hydrogenation.

6. Conclusions

We presented a comparative study of formyl adsorption on surfaces of Pd, Cu, and PdZn. The computational results were obtained by applying a DF method to periodic slab models. CHO binds least strongly at Cu(111) ($\Delta E_{ad} = -127$ kJ mol^{-1}) and strongest at Pd(111) ($\Delta E_{ad} = -214$ kJ mol^{-1}). The energies of adsorption ΔE_{ad} of formyl on PdZn(111) and PdZn(221), -167 and -186 kJ mol^{-1}, respectively, were determined to be intermediate between those on Pd and Cu. All potential energy surfaces of formyl adsorption were judged to be rather flat; the energies of adsorption ΔE_{ad} of several key adsorption sites vary by less than 15 kJ mol^{-1}. This implies easy diffusion of formyl on the surfaces of Pd, Cu, and PdZn.

We also characterized computationally both the thermodynamics and the kinetics of formaldehyde and formyl dehydrogenation on these surfaces. Calculated activation energies show that dehydrogenation of formaldehyde is favorable on Pd(111), but unfavorable on the surfaces of Cu and PdZn alloy. We rationalized the experimentally observed formation of CO on PdZn alloy by formaldehyde dehydrogenation at monometallic Pd sites or at PdZn alloy defect sites of the Pd/ZnO catalyst. Optimization of Pd loading on ZnO catalyst appears to be required to ensure that during methanol steam reforming on the Pd/ZnO catalyst the amount of undesirable CO byproduct is minimized.

Finally, we discussed implications of our results on CO hydrogenation to methanol. The initial step of this reaction is both kinetically and thermodynamically unfavorable on the substrates studied, in agreement with experimental evidence that methanol is not formed on Pd and Pd/ZnO catalysts by means of CO hydrogenation.[41]

Acknowledgment. K.H.L. is grateful to the Deutscher Akademischer Austauschdienst for a fellowship. Z.-X.C. thanks

the Alexander von Humboldt Foundation for a fellowship. This work was supported by the Deutsche Forschungsgemeinschaft, Fonds der Chemischen Industrie (Germany), the Spanish Ministry of Education and Science (Grant CTQ2005-08459-C02-01), and the Generalitat de Catalunya (2005SGR00697).

Supporting Information Available: Cartesian coordinates and vibrational frequencies of pertinent structures are given. This material is available free of charge via the Internet at http://pubs.acs.org.

References and Notes

(1) Holladay, J. D.; Wang, Y.; Jones, E. *Chem. Rev.* **2004**, *104*, 4767.
(2) Takezawa, N.; Iwasa, N. *Catal. Today* **1997**, *36*, 45.
(3) Cubeiro, M. L.; Fierro, J. L. G. *J. Catal.* **1998**, *179*, 150.
(4) Pfeifer, P.; Schubert, K.; Liauw, M. A.; Emig, G. *Appl. Catal. A* **2004**, *270*, 165.
(5) Iwasa, N.; Mayanagi, T.; Masuda, S.; Takezawa, N. *React. Kinet. Catal. Lett.* **2000**, *69*, 355.
(6) Iwasa, N.; Takezawa, N. *Top. Catal.* **2003**, *22*, 215.
(7) Suwa, Y.; Ito, S.; Kameoka, S.; Tomishige, K.; Kunimori, K. *Appl. Catal. A* **2004**, *267*, 9.
(8) Choudhary, T. V.; Goodman, D. W. *Catal. Today* **2002**, *77*, 65.
(9) Chen, Z.-X.; Neyman, K. M.; Gordienko, A. B.; Rösch, N. *Phys. Rev. B* **2003**, *68*, 7514.
(10) Chen, Z.-X.; Neyman, K. M.; Rösch, N. *Surf. Sci.* **2004**, *548*, 291.
(11) Neyman, K. M.; Sahnoun, R.; Inntam, C.; Hengrasmee, S.; Rösch, N. *J. Phys. Chem. B* **2004**, *108*, 5424.
(12) Bayer, A.; Flechtner, K.; Denecke, R.; Steinrück, H.-P.; Neyman, K. M.; Rösch, N. *Surf. Sci.* **2006**, *600*, 78.
(13) Chen, Z.-X.; Neyman, K. M.; Lim, K. H.; Rösch, N. *Langmuir* **2004**, *20*, 8068.
(14) Chen, Z.-X.; Lim, K. H.; Neyman, K. M.; Rösch, N. *Phys. Chem. Chem. Phys.* **2004**, *6*, 4499.
(15) Chen, Z.-X.; Lim, K. H.; Neyman, K. M.; Rösch, N. *J. Phys. Chem. B* **2005**, *109*, 4568.
(16) Lee, J. K.; Ko, J. B.; Kim, D. H. *Appl. Catal. A* **2004**, *278*, 25.
(17) Greeley, J.; Mavrikakis, M. *J. Catal.* **2002**, *208*, 291.
(18) Neurock, M. *Top. Catal.* **1999**, *9*, 135.
(19) Perdew, J. P.; Wang, Y. *Phys. Rev. B* **1992**, *45*, 13244.
(20) Becke, A. D. *Phys. Rev. A* **1988**, *38*, 3098.
(21) Perdew, J. P. *Phys. Rev. B* **1986**, *33*, 8622; *Phys. Rev. B* **1986**, *34*, 7406.
(22) Kresse, G.; Furthmüller, J. *Phys. Rev. B* **1996**, *54*, 11169.
(23) Kresse, G.; Hafner, J. *Phys. Rev. B* **1993**, *47*, 558.
(24) Kresse, G.; Furthmüller, J. *Comput. Mater. Sci.* **1999**, *6*, 15.
(25) Blöchl, P. E. *Phys. Rev. B* **1994**, *50*, 17953.
(26) Kresse, G.; Joubert, D. *Phys. Rev. B* **1999**, *59*, 1758.
(27) Monkhorst, H. J.; Pack, J. D. *Phys. Rev. B* **1976**, *13*, 5188.
(28) Methfessel, M.; Paxton, A. T. *Phys. Rev. B* **1989**, *40*, 3616.
(29) Mills, G.; Jónsson, H.; Schenter, G. K. *Surf. Sci.* **1995**, *324*, 305.
(30) Greeley, J.; Mavrikakis, M. *J. Phys. Chem. B* **2005**, *109*, 3460.
(31) Desai, S. K.; Neurock, M.; Kourtakis, K. *J. Phys. Chem. B* **2002**, *106*, 2559.
(32) Greeley, J.; Mavrikakis, M. *J. Am. Chem. Soc.* **2004**, *126*, 3910.
(33) Gomes, J. R. B.; Gomes, J. A. N. F. *J. Electroanal. Chem.* **2000**, *483*, 180.
(34) Papoian, G.; Nørskov, J. K.; Hoffmann, R. *J. Am. Chem. Soc.* **2000**, *122*, 4129.
(35) Alavi, A.; Hu, P. J.; Deutsch, T.; Silverstrelli, P. L.; Hutter, J. *Phys. Rev. Lett.* **1998**, *80*, 3650.
(36) Lim, K. H. Doctoral Thesis, Technische Universität München, 2006.
(37) Sexton, B. A. *Surf. Sci.* **1981**, *102*, 271.
(38) Russell, J. N., Jr.; Gates, S. M.; Yates, J. T., Jr. *Surf. Sci.* **1985**, *163*, 516.
(39) Liu, S. T.; Takahashi, K.; Uematsu, K.; Ayabe, M. *Appl. Catal. A* **2005**, *283*, 125.
(40) Askgaard, T. S.; Nørskov, J. K.; Ovesen, C. V.; Stoltze, P. *J. Catal.* **1995**, *156*, 229.
(41) Iwasa, N.; Suzuki, H.; Terracita, M.; Arai, M.; Takezawa, N. *Catal. Lett.* **2004**, *96*, 75.